

Permafrost, Lakes, and Climate-Warming Methane Feedback: What is the Worst We Can Expect?

Xiang Gao, C. Adam Schlosser, Andrei Sokolov,
Katey Walter Anthony, Qianlai Zhuang and David Kicklighter



Report No. 218
May 2012

The MIT Joint Program on the Science and Policy of Global Change is an organization for research, independent policy analysis, and public education in global environmental change. It seeks to provide leadership in understanding scientific, economic, and ecological aspects of this difficult issue, and combining them into policy assessments that serve the needs of ongoing national and international discussions. To this end, the Program brings together an interdisciplinary group from two established research centers at MIT: the Center for Global Change Science (CGCS) and the Center for Energy and Environmental Policy Research (CEEPR). These two centers bridge many key areas of the needed intellectual work, and additional essential areas are covered by other MIT departments, by collaboration with the Ecosystems Center of the Marine Biology Laboratory (MBL) at Woods Hole, and by short- and long-term visitors to the Program. The Program involves sponsorship and active participation by industry, government, and non-profit organizations.


To inform processes of policy development and implementation, climate change research needs to focus on improving the prediction of those variables that are most relevant to economic, social, and environmental effects. In turn, the greenhouse gas and atmospheric aerosol assumptions underlying climate analysis need to be related to the economic, technological, and political forces that drive emissions, and to the results of international agreements and mitigation. Further, assessments of possible societal and ecosystem impacts, and analysis of mitigation strategies, need to be based on realistic evaluation of the uncertainties of climate science.

This report is one of a series intended to communicate research results and improve public understanding of climate issues, thereby contributing to informed debate about the climate issue, the uncertainties, and the economic and social implications of policy alternatives. Titles in the Report Series to date are listed on the inside back cover.

Ronald G. Prinn and John M. Reilly
Program Co-Directors

For more information, please contact the Joint Program Office

Postal Address: Joint Program on the Science and Policy of Global Change
77 Massachusetts Avenue
MIT E19-411
Cambridge MA 02139-4307 (USA)
Location: 400 Main Street, Cambridge
Building E19, Room 411
Massachusetts Institute of Technology
Access: Phone: +1.617. 253.7492
Fax: +1.617.253.9845
E-mail: globalchange@mit.edu
Web site: <http://globalchange.mit.edu/>

 Printed on recycled paper

Permafrost, Lakes, and Climate-Warming Methane Feedback: What is the Worst We Can Expect?

Xiang Gao^{1†}, C. Adam Schlosser¹, Andrei Sokolov¹, Katey Walter Anthony², Qianlai Zhuang³,
and David Kicklighter⁴

Abstract

Permafrost degradation is likely enhanced by climate warming. Subsequent landscape subsidence and hydrologic changes support expansion of lakes and wetlands. Their anaerobic environments can act as strong emission sources of methane and thus represent a positive feedback to climate warming. Using an integrated earth-system model framework, which considers the range of policy and uncertainty in climate-change projections, we examine the influence of near-surface permafrost thaw on the prevalence of lakes, its subsequent methane emission, and potential feedback under climate warming. We find that increases in atmospheric CH₄ and radiative forcing from increased lake CH₄ emissions are small, particularly when weighed against unconstrained human emissions. The additional warming from these methane sources, across the range of climate policy and response, is no greater than 0.1°C by 2100. Further, for this temperature feedback to be discernable by 2100 would require at least an order of magnitude larger methane-emission response. Overall, the biogeochemical climate-warming feedback from boreal and Arctic lake emissions is relatively small whether or not humans choose to constrain global emissions.

Contents

1. INTRODUCTION.....	1
2. MODELS AND METHOD	2
3. RESULTS AND ANALYSIS	3
3.1 Trends in Near-surface Permafrost Extents	3
3.2 Trends in Saturated Area/ Lake Extent.....	4
3.3 Methane Emission from Lake Expansion	5
3.4 Climate Feedback	6
4. DISCUSSIONS AND CONCLUSIONS.....	8
5. REFERENCES	8
APPENDIX A: Downscaling Scheme	12
APPENDIX B: Temperature Dependence of Methane Ebullition Flux.....	13
APPENDIX C: IGSM Estimated Human Global CH ₄ Emissions	14
APPENDIX D.....	15

1. INTRODUCTION

Arctic and boreal permafrost represent significant yet vulnerable carbon reservoirs (Zimov *et al.*, 2006; Schuur *et al.*, 2008). There is general agreement that 21st century warming would be pronounced at higher latitudes (Solomon *et al.*, 2007). Considerable concern has been placed on the permafrost in near-surface, ice-rich soils (Lawrence and Slater, 2005; Jorgenson *et al.*, 2006; Zhang *et al.*, 2008) as thaw-inducing temperature increases can cause landscape subsidence as well as sub-surface hydrologic change and thus form saturated areas such as thermokarst lakes

¹ Joint Program on the Science and Policy of Global Change, Massachusetts Institute of Technology, Cambridge, MA.

² Water and Environmental Research Center, University of Alaska Fairbanks, Fairbanks, AK.

³ Departments of Earth & Atmospheric Science and Agronomy, Purdue University, West Lafayette, IN.

⁴ The Ecosystems Center, Marine Biology Laboratory, Woods Hole, MA.

[†] Corresponding author (Email: xgao304@mit.edu)

and wetlands. Subsequently, anaerobic decomposition of thawed organic carbon results in emission of methane, a potent greenhouse gas, which could fuel a positive feedback to the global climate system (Walter *et al.*, 2006, 2007b; Zimov *et al.*, 1997; McGuire *et al.*, 2006; Anisimov, 2007; Shindell *et al.*, 2004). Permafrost thaw also strongly influences local hydrology, vegetation composition, ecosystem functioning as well as surface albedo and surface-energy partitioning (Smith *et al.*, 2005; Jorgenson *et al.*, 2001; Christensen *et al.*, 2004).

2. MODELS AND METHOD

We use the MIT Integrated Global System Model (IGSM) that allows for quantifying uncertainties in projected future climates (Sokolov *et al.*, 2005). In the IGSM, we employ the Community Land Model (CLM) version 3.5 (Oleson *et al.*, 2008) to: estimate near-surface permafrost extent; project permafrost degradation; quantify methane emissions fueled by subsequent lake expansion; and assess the extent these emissions provide a feedback to global climate warming. The atmospheric data that drive CLM are from the IGSM transient 20th and 21st century climate-change integration (Sokolov *et al.*, 2009; Webster *et al.*, 2012). Further, the simulation framework accounts for uncertainties in: the transient climate response (TCR) that aggregates the effect of three climate parameters (climate sensitivity, rate of ocean heat uptake, and aerosol forcing); emissions under climate policy goals; and regional climate change.

Table 1. Summary of Simulation Experiments Conducted in This Study.

<i>Unconstrained Emission (UCE)</i>			
TCR	Emission	Notes	Abbreviation
High (95%)	Median (1330 ppm CO ₂ -Eq)	+17 regional patterns	HTCR
Median (50%)		Baseline	MTCR
Low (5%)		+17 regional patterns	LTCR
Median (50%)	High (95%) (1660 ppm CO ₂ -Eq)		MTCR_HEM
	Low (95%) (970 ppm CO ₂ -Eq)		MTCR_LEM
<i>Greenhouse-gas Stabilization (GST)</i>			
TCR	Emission	Notes	Abbreviation
High (95%)	560 ppm CO ₂ -Eq	+17 regional patterns	H560
Low (5%)		+17 regional patterns	L560

The IGSM sub-model of atmospheric dynamics and chemistry is 2-dimensional (2D) in altitude and latitude and coupled to a mixed-layer ocean (Sokolov *et al.*, 2005). Yet, the IGSM consistently depicts the global and zonal profiles of climate change when compared with the Intergovernmental Panel on Climate Change (IPCC) 4th Assessment Report (AR4) archive (Sokolov *et al.*, 2009; Webster *et al.*, 2012; Schlosser *et al.*, 2012). The suite of simulations encompasses the range in emission pathways (an unconstrained and stabilization emission

scenario) as well as the large-scale climate response (**Table 1**). Parameter values were chosen to produce the high (95%), median (50%), and low (5%) TCR response of a 400-member ensemble simulation (Webster *et al.*, 2012). A downscaling technique (Schlosser *et al.*, 2012) expands the IGSM zonal near-surface meteorology (precipitation, surface air temperature, and radiation) to generate corresponding longitudinal patterns (Appendix A). Climatology of these patterns is derived from observations (Huffman *et al.*, 2009; Mitchell and Jones, 2005; Ngo-Duc *et al.*, 2005; Qian *et al.*, 2006; Betts *et al.*, 2006), and pattern shifts in response to human-forced change are based on climate-model results from the IPCC AR4 archive (Schlosser *et al.*, 2012). As such, the uncertainty in regional climate change can be considered. With these meteorological variables, CLM simulations (Table 1) of the 21st century were conducted at a 2° by 2.5° resolution to assess potential shifts in permafrost/lake extent and corresponding emissions of methane.

3. RESULTS AND ANALYSIS

3.1 Trends in Near-surface Permafrost Extents

Each model grid, having a 3.5 meter soil-column depth, is identified as containing permafrost if monthly soil temperature in at least one subsurface soil layer remains at or below 0°C for two or more consecutive years. Given this, we simulate a near-surface (down to 3.5 meter below the surface) permafrost area (poleward of 45°N and excluding glacial regions) of $11.2 \times 10^6 \text{ km}^2$ from 1970 to 1989, which falls on the lower bound of the observationally based range of continuous

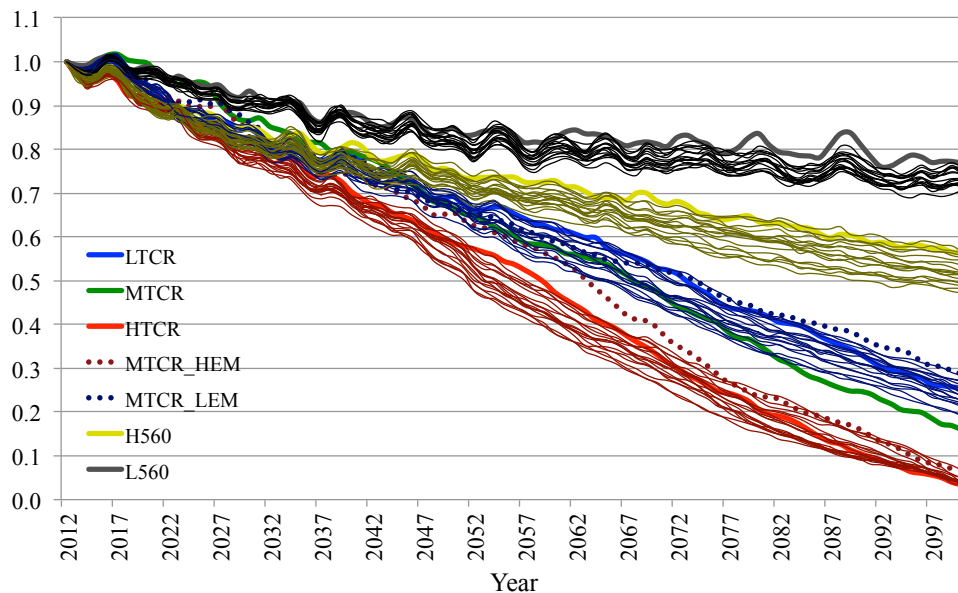


Figure 1. Fractional change in the total area containing near-surface permafrost (NSP) (poleward of 45°N and excluding glacial regions) with respect to 2012 (around $1.02 \times 10^{13} \text{ m}^2$) under various climate projections. Thick solid lines represent the use of climatological geographic patterns in precipitation, temperature, and radiation throughout the 21st century. Thin solid lines represent the inclusion of additional model-dependent geographic pattern shifts in precipitation, temperature, and radiation derived from the IPCC AR4 climate model projections throughout the 21st century. The definition of figure legend is detailed in Table 1.

and discontinuous permafrost extent (11.2 to $13.5 \times 10^6 \text{ km}^2$) over the same period (Zhang *et al.*, 2000). Through the 21st century, the simulations indicate a nearly linear near-surface permafrost (NSP) degradation rate, with the potential for 75% loss for the low TCR and nearly 100% loss for the high TCR cases by 2100 under an unconstrained emissions scenario (UCE) (**Figure 1**). We also find that uncertainty in emissions (dotted lines) are as important as climate-response uncertainty (thick solid lines), in terms of contributing to the total uncertainty in projected NSP changes. Under a greenhouse-gas stabilization target (GST) scenario of 560 ppm CO₂-equivalent concentration by 2100 (Webster *et al.*, 2012), NSP degradation reduces substantially, with 20% loss for low TCR and 40% loss for high TCR by 2100. Compared with previous work (Lawrence *et al.*, 2008), our simulated NSP loss rate through the 21st century is somewhat slower. In addition, uncertain regional climate change (Figure 1, thin lines) may accelerate the NSP thaw by 5% ~10% due to enhanced warming over land imposed by the climate-model patterns (Schlosser *et al.*, 2012).

3.2 Trends in Saturated Area/ Lake Extent

From these NSP projections, we next determine the potential lake methane-emission increase and climate-warming feedback. To characterize an upper-limit to this feedback, we draw from previous work (Gedney *et al.*, 2004) and interpret the models diagnoses of a change in land area where the water table has reached the ground surface (or saturated land area) as a concurrent and equal increase in lake area. This interpretation, clearly, approximates the true fate of future lake extent. Indeed, the intent here is not to provide a deterministic prediction, but rather, the maximum lake expansion anticipated under these model projections. Further considerations are discussed in the closing section. Nevertheless, the model explicitly accounts for the major

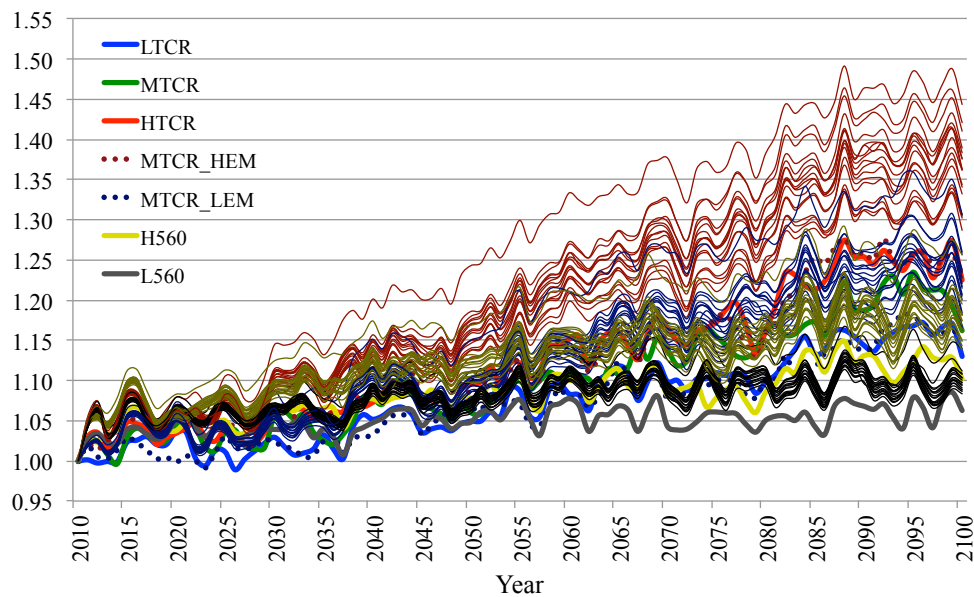


Figure 2. Same as Figure 1, but for the total saturated area (poleward of 45°N and excluding glacier) with respect to 2010. The total saturated area at 2010 is estimated to be around $7.73 \times 10^{11} \text{ m}^2$.

hydrologic and topographic controls of water table variations (for an unconfined aquifer). By this measure, modeled lake area north of 45°N (excluding glacier) increases 15% to 25% by 2100 for the low and high TCR response, respectively, under the UCE scenario (**Figure 2**). Under the GST scenario, the expansion of lakes is limited to 5% and 15%, respectively. Uncertain regional climate-change can enhance lake expansion, especially for the UCE scenario and high TCR, causing a 30% to 50% increase by 2100 (Figure 2, thin red lines). Overall, the total estimated lake area increases from 5% to 50% by 2100 across all the projections.

3.3 Methane Emission from Lake Expansion

To convert our inferred lake-area expansion into CH₄ emission estimates, we account for a key distinction: yedoma versus non-yedoma (Walter *et al.*, 2006; Walter Anthony *et al.*, 2012). Yedoma regions are underlain by organic-rich Pleistocene-age soil with ice content typically from 50% to 90% by volume (Walter *et al.*, 2006; Zimov *et al.*, 1997), and measurements taken at yedoma lakes show significantly higher ebullition CH₄ fluxes than non-yedoma counterparts (Walter *et al.*, 2006; Walter Anthony *et al.*, 2012). From these field measurements, we can directly infer a corresponding CH₄ flux from our estimated lake-area expansion (Appendix B). We pool all measured CH₄ fluxes into yedoma and non-yedoma categories, based on their

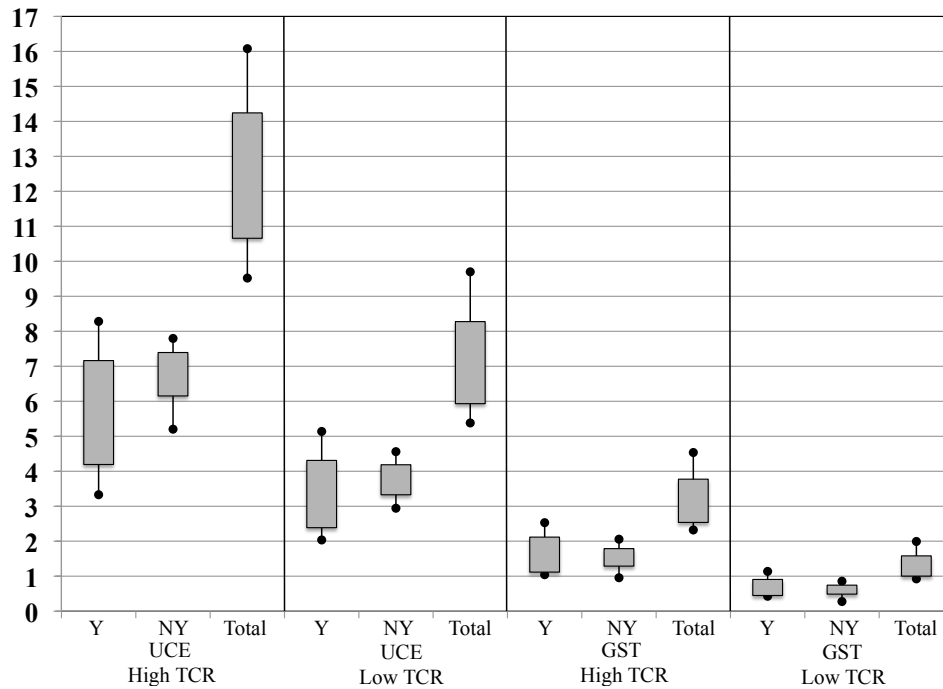


Figure 3. Increases in decadal averaged (2091-2100) annual CH₄ emission (Tg-CH₄yr⁻¹, poleward of 45°N) with respect to 2011-2020 as a result of the expansion of yedoma lakes (Y), non-yedoma (NY) lakes, and all lakes for the low and high TCR cases under the UCE and GST scenarios, respectively. Each scenario contains a total of 18 ensemble members (17 members of model-based pattern shifts and one member of climatological pattern). Whisker plots show the minimum, maximum, and plus/minus one standard deviation about the ensemble mean.

location with respect to a contemporary atlas of yedoma regions (Walter *et al.*, 2007a). Average yedoma and non-yedoma lake methane-flux values are obtained from these pooled measurements. These representative CH₄ fluxes are then applied to each model grids simulated lake-area expansion according to whether the grid lies over a dominantly covered yedoma or non-yedoma zone. Their product results in an emission rate for that grid. Additionally, a Q₁₀ relation (Appendix B) approximates the lake sediment temperature dependency of microbial activity leading to ebullition flux. By this method, we estimate an average annual CH₄ emission of 6.8 Tg-CH₄yr⁻¹ from lakes poleward of 45°N from 2011 to 2020, which falls within the range of the previous estimates (Walter *et al.*, 2007b; Huissteden *et al.*, 2011). By the end of the 21st century, under the UCE scenario, increases in decadal averaged (2091-2100) annual CH₄ emission from lake expansion range between 5.4 to 9.7 Tg-CH₄yr⁻¹ (79% to 143% increase) and 9.5 to 16.1 Tg-CH₄yr⁻¹ (140% to 237% increase) for the low and high TCR cases, respectively, of which approximately 50% is contributed by yedoma lake expansion (**Figure 3**). Nevertheless, these changes are considerably lower than the IGSM estimated human global CH₄ emission increase of 349 Tg-CH₄yr⁻¹ (Appendix C). Under the GST scenario, the CH₄ emission increases by 2100 are substantially lower relative to the UCE scenario. The decadal averaged annual emission increases are 0.9 to 2.0 Tg-CH₄yr⁻¹ (13% to 29% increase) and 2.3 to 4.5 Tg-CH₄yr⁻¹ (34% to 66% increase) for the low and high TCR cases, respectively. However, unlike the UCE scenario, these increases are comparable to the corresponding IGSM estimated global CH₄ human-emission increase at 4 Tg-CH₄yr⁻¹ (Appendix C).

3.4 Climate Feedback

To assess the potential climate-warming feedback from the increased lake emissions, we then run the IGSM and exogenously prescribe the aforementioned lake CH₄ flux increases through the 21st century. For the UCE scenario, the ensemble-mean result shows no discernable temperature feedback as the increases in anthropogenic emissions overwhelm the lake emission increase (not shown). For the ensemble-mean of the GST scenario, no salient global surface-air temperature feedback is discernable for either the high or low TCR case in response to the added lake CH₄ emission (**Figure 4a**). Among all the simulations performed (Table 1), only one member of the model ensemble exhibits a small temperature feedback of approximately 0.1°C towards the end of this century (not shown), although the salient additional warming is somewhat overshadowed by interannual variability. Although the range of the end-of-century increase in lake CH₄ emission (0.9 to 4.5 Tg-CH₄yr⁻¹ is comparable to the human-emission increase (4 Tg-CH₄yr⁻¹) under the GST scenario, it is still quite low (on the order of 1%) when compared with the current level of human emission rates (345 Tg-CH₄yr⁻¹ at 2010, Appendix C), and particularly when considering all greenhouse gas emissions. Further IGSM tests indicate that a 1% increase of CH₄ concentration, consistent with the aforementioned CH₄ flux increases, has a very minor effect on radiative forcing (Appendix D).

To characterize the relative scale of the derived CH₄ lake-emission response, particularly with respect to additional CH₄ emissions needed for a more salient climate-warming feedback, we

perform sensitivity experiments by augmenting the CH₄ emissions and repeating the 21st century IGSM projections. Each run separately considers: scaling the CH₄ lake-emission increases by 10, 25, 50 and 100-fold; and applying only the CH₄ human-emission increases of the UCE scenario. Notable results are obtained for the GST scenario at the high TCR. The results (**Figure 4b**) indicate the 10-fold increase would not support a salient temperature-feedback response. The

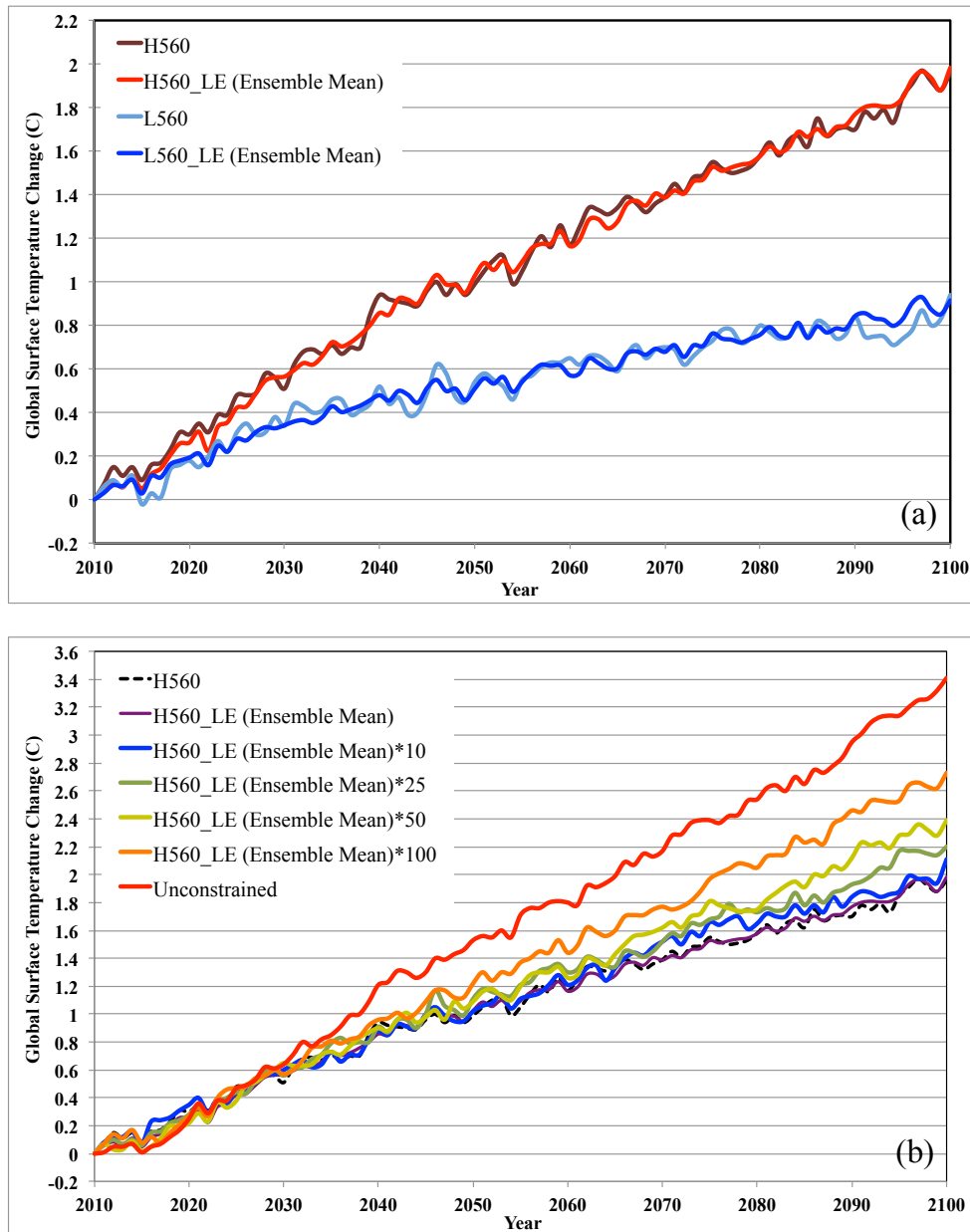


Figure 4. a) Global temperature feedback from the increased lake CH₄ emissions for the low and high TCR cases under the GST scenario. LE in the legend refers to the lake emission. b) The sensitivity of global temperature change (°C) to the increased lake CH₄ emission for the high TCR case under the GST scenario. *10, *25, *50, and *100 refer to the experiments with the CH₄ lake-emission increases scaled by 10, 25, 50 and 100-fold, respectively. Also shown is the global temperature change by applying only the CH₄ human-emission increases of the UCE scenario.

100-fold increase produces a temperature response of about 0.8°C by 2100, but salient only after mid-century. The UCE human CH₄ emission increases cause temperature to rise about 1.5°C by 2100. However, at a 25-fold lake-emission increase, the model exhibits a discernable, additional warming of 0.2°C, but evident only in the last decade of the 21st century.

4. DISCUSSIONS AND CONCLUSIONS

Overall, these results present, for the first time, a quantitative insight on the scale of the climate-warming feedback from permafrost thaw and subsequent CH₄ lake emission. The increase in CH₄ emission due to potential Arctic/boreal lake expansion represents a weak climate-warming feedback within this century. This is consistent with previous studies (Anisimov, 2007; Huissteden *et al.*, 2011; Delisle, 2007) that also imply a small Arctic lake/wetland biogeochemical climate-warming feedback. Our experimental design does not explicitly consider the wetlands potential CH₄-emissions response (Shindell *et al.*, 2004). As previously noted, the additional saturated area projected by our model is characterized to be lake in terms of a CH₄ emission source (to gauge an upper bound). Yet, in this way, if any presumed, additional lake area would alternatively be wetland, to first order we still account for this in terms of a CH₄-emission response. Our lake identification scheme also does not explicitly consider lake thermodynamics or thermo-geomorphologic distinction (e.g. thermokarst). Further, buffering effects from near-surface drainage (Huissteden *et al.*, 2011; Avis *et al.*, 2011) are not explicitly considered, however these drainage effects would further weaken the already small feedback found. Other secondary factors not explicitly considered in this study include: the insulating properties of soil organic matter (Lawrence *et al.*, 2008), the response of CH₄ emission to soil-moisture dynamics, fire disturbance, vegetation dynamics, as well as lake freeze-depth. Nevertheless, these considerations will likely not change our overall conclusion: the biogeochemical climate-warming feedback via boreal and Arctic lake methane emissions is relatively small, whether or not humans choose to constrain global emissions.

Acknowledgements

This work was supported under the Department of Energy Climate Change Prediction Program Grant DE-PS02-08ER08-05. The authors gratefully acknowledge this as well as additional financial support provided by the MIT Joint Program on the Science and Policy of Global Change through a consortium of industrial sponsors and Federal grants. Development of the IGSM applied in this research is supported by the U.S. Department of Energy, Office of Science (DE-FG02-94ER61937); the U.S. Environmental Protection Agency, EPRI, and other U.S. government agencies and a consortium of 40 industrial and foundation sponsors. For a complete list see <http://globalchange.mit.edu/sponsors/current.html>.

5. REFERENCES

- Anisimov, O. A., 2007: Potential feedback of thawing permafrost to the global climate system through methane emission. *Environmental Research Letters*, **2**(4): 045016.
doi:10.1088/1748-9326/2/4/045016.
- Avis, C. A., A. J. Weaver and K. J. Meissner, 2011: Reduction in areal extent of high-latitude

- wetlands in response to permafrost thaw. *Nature Geoscience*, **4**(7): 444–448. doi:[10.1038/NGEO1160](https://doi.org/10.1038/NGEO1160).
- Betts, A. K., M. Zhao, P. A. Dirmeyer and A. C. M. Beljaars, 2006: Comparison of ERA40 and NCEP/DOE near-surface data sets with other ISLSCP-II data sets. *Journal of Geophysical Research-Atmospheres*, **111**(D22): D22S04. doi:[10.1029/2006JD007174](https://doi.org/10.1029/2006JD007174).
- Christensen, T. R., T. R. Johansson, H. J. Akerman, M. Mastepanov, N. Malmer, T. Friborg, P. Crill and B. H. Svensson, 2004: Thawing sub-arctic permafrost: Effects on vegetation and methane emissions. *Geophysical Research Letters*, **31**(4): L04501. doi:[10.1029/2003GL018680](https://doi.org/10.1029/2003GL018680).
- Delisle, G., 2007: Near-surface permafrost degradation: How severe during the 21st century? *Geophysical Research Letters*, **34**(9): L09503. doi:[10.1029/2007GL029323](https://doi.org/10.1029/2007GL029323).
- Gedney, N., P. M. Cox and C. Huntingford, 2004: Climate feedback from wetland methane emissions. *Geophysical Research Letters*, **31**(20): L20503. doi:[10.1029/2004GL020919](https://doi.org/10.1029/2004GL020919).
- Huffman, G. J., R. F. Adler, D. T. Bolvin and G. Gu, 2009: Improving the global precipitation record: GPCP Version 2.1. *Geophysical Research Letters*, **36**: L17808. doi:[10.1029/2009GL040000](https://doi.org/10.1029/2009GL040000).
- Huissteden, J. V., C. Berrittella, F. J. W. Parmentier, Y. Mi, T. C. Maximov and A. J. Dolman, 2011: Methane emissions from permafrost thaw lakes limited by lake drainage. *Nature Climate Change*, **1**(2): 119–123. doi:[10.1038/NCLIMATE1101](https://doi.org/10.1038/NCLIMATE1101).
- Jorgenson, M. T., C. H. Racine, J. C. Walters and T. E. Osterkamp, 2001: Permafrost degradation and ecological changes associated with a warming climate in central Alaska. *Climatic Change*, **48**(4): 551–579.
- Jorgenson, M. T., Y. L. Shur and E. R. Pullman, 2006: Abrupt increase in permafrost degradation in Arctic Alaska. *Geophysical Research Letters*, **33**(2): L02503. doi:[10.1029/2005GL024960](https://doi.org/10.1029/2005GL024960).
- Lawrence, D. M. and A. G. Slater, 2005: A projection of severe near-surface permafrost degradation during the 21st century. *Geophysical Research Letters*, **32**(24): L24401. doi:[10.1029/2005GL025080](https://doi.org/10.1029/2005GL025080).
- Lawrence, D. M., A. G. Slater, V. E. Romanovsky and D. J. Nicolsky, 2008: Sensitivity of a model projection of near-surface permafrost degradation to soil column depth and representation of soil organic matter. *Journal of Geophysical Research-Earth Surface*, **113**(F2): F02011. doi:[10.1029/2007JF000883](https://doi.org/10.1029/2007JF000883).
- McGuire, A. D., F. S. I. Chapin, J. E. Walsh and C. Wirth, 2006: Integrated regional changes in arctic climate feedbacks: Implications for the global climate system. *Annual Review of Environment and Resources*, **31**: 61–91. doi:[10.1146/annurev.energy.31.020105.100253](https://doi.org/10.1146/annurev.energy.31.020105.100253).
- Mitchell, T. D. and P. D. Jones, 2005: An improved method of constructing a database of monthly climate observations and associated high-resolution grids. *International Journal of Climatology*, **25**(6): 693–712. doi:[10.1002/joc.1181](https://doi.org/10.1002/joc.1181).
- Ngo-Duc, T., J. Polcher and K. Laval, 2005: A 53-year forcing data set for land surface models. *Journal of Geophysical Research-Atmospheres*, **110**(D6): D06116. doi:[10.1029/2004JD005434](https://doi.org/10.1029/2004JD005434).

- Oleson, K. W., G. Y. Niu, Z. L. Yang, D. M. Lawrence, P. E. Thornton, P. J. Lawrence, R. Stoeckli, R. E. Dickinson, G. B. Bonan, S. Levis, A. Dai and T. Qian, 2008: Improvements to the Community Land Model and their impact on the hydrological cycle. *Journal of Geophysical Research-Biogeosciences*, **113**(G1): G01021. doi:[10.1029/2007JG000563](https://doi.org/10.1029/2007JG000563).
- Qian, T., A. Dai, K. E. Trenberth and K. W. Oleson, 2006: Simulation of global land surface conditions from 1948 to 2004. Part I: Forcing data and evaluations. *Journal of Hydrometeorology*, **7**(5): 953–975.
- Schlosser, C. A., X. Gao, K. Strzepak, A. P. Sokolov, C. Forest, S. Awadalla, W. Farmer and H. D. Jacoby, 2012: Quantifying the likelihood of regional climate change: a hybridized approach. *Journal of Climate*.
- Schuur, E. A. G., J. Bockheim, J. G. Canadell, E. Euskirchen, C. B. Field, S. V. Goryachkin, S. Hagemann, P. Kuhry, P. M. Lafleur, H. Lee, G. Mazhitova, F. E. Nelson, A. Rinke, V. E. Romanovsky, N. Shiklomanov, C. Tarnocai, S. Venevsky, J. G. Vogel and S. A. Zimov, 2008: Vulnerability of permafrost carbon to climate change: Implications for the global carbon cycle. *Bioscience*, **58**(8): 701–714. doi:[10.1641/B580807](https://doi.org/10.1641/B580807).
- Shindell, D. T., B. P. Walter and G. Faluvegi, 2004: Impacts of climate change on methane emissions from wetlands. *Geophysical Research Letters*, **31**(21): L21202. doi:[10.1029/2004GL021009](https://doi.org/10.1029/2004GL021009).
- Smith, L. C., Y. Sheng, G. M. MacDonald and L. D. Hinzman, 2005: Disappearing Arctic lakes. *Science*, **308**(5727): 1429–1429. doi:[10.1126/science.1108142](https://doi.org/10.1126/science.1108142).
- Sokolov, A. P., C. A. Schlosser, S. Dutkiewicz, S. Paltsev, D. Kicklighter, H. Jacoby, R. Prinn, C. Forest, J. Reilly, C. Wang, B. Felzer, M. Sarofim, J. Scott, P. Stone, J. Melillo and J. Cohen, 2005: The MIT Integrated Global System Model (IGSM) Version 2: Model description and baseline evaluation. MIT JPSPGC Report 124, July, 40 p. (http://globalchange.mit.edu/files/document/MITJPSPGC_Rpt124.pdf).
- Sokolov, A. P., P. H. Stone, C. E. Forest, R. Prinn, M. C. Sarofim, M. Webster, S. Paltsev, C. A. Schlosser, D. Kicklighter, S. Dutkiewicz, J. Reilly, C. Wang, B. Felzer, J. M. Melillo and H. D. Jacoby, 2009: Probabilistic Forecast for Twenty-First-Century Climate Based on Uncertainties in Emissions (Without Policy) and Climate Parameters. *Journal of Climate*, **22**(19): 5175–5204. doi:[10.1175/2009JCLI2863.1](https://doi.org/10.1175/2009JCLI2863.1).
- Solomon, S., D. Qin, M. Manning, Z. Chen, M. Marquis, K. Averyt, M. Tignor and H. Miller, 2007: Contribution of Working Group I to the Fourth Assessment Report of the Intergovernmental Panel on Climate Change. *Cambridge University Press, Cambridge, United Kingdom and New York*.
- Walter, K. M., S. A. Zimov, J. P. Chanton, D. Verbyla and F. S. I. Chapin, 2006: Methane bubbling from Siberian thaw lakes as a positive feedback to climate warming. *Nature*, **443**(7107): 71–75. doi:[10.1038/nature05040](https://doi.org/10.1038/nature05040).
- Walter, K. M., M. E. Edwards, G. Grosse, S. A. Zimov and F. S. I. Chapin, 2007a: Thermokarst lakes as a source of atmospheric CH₄ during the last deglaciation. *Science*, **318**(5850): 633–636. doi:[10.1126/science.1142924](https://doi.org/10.1126/science.1142924).

- Walter, K. M., L. C. Smith and F. S. I. Chapin, 2007b: Methane bubbling from northern lakes: present and future contributions to the global methane budget. *Philosophical Transactions of the Royal Society A-Mathematical Physical and Engineering Sciences*, **365**(1856): 1657–1676. doi:[10.1098/rsta.2007.2036](https://doi.org/10.1098/rsta.2007.2036).
- Walter Anthony, K. M., P. Anthony, G. Grosse and J. Chanton, 2012: Geologic methane seeps along boundaries of arctic permafrost thaw and melting glaciers. *Nature Geoscience*.
- Webster, M., A. P. Sokolov, J. M. Reilly, C. E. Forest, S. Paltsev, C. A. Schlosser, C. Wang, D. Kicklighter, M. Sarofim, J. Melillo, R. G. Prinn and H. D. Jacoby, 2012: Analysis of climate policy targets under uncertainty. *Climatic Change*, (10.1007/s10584-011-0260-0).
- Zhang, T., J. A. Heginbottom, R. G. Barry and J. Brown, 2000: Further statistics on the distribution of permafrost and ground-ice in the Northern Hemisphere. *Polar Geogr.*, **24**: 126–131.
- Zhang, Y., W. Chen and D. W. Riseborough, 2008: Transient projections of permafrost distribution in Canada during the 21st century under scenarios of climate change. *Global and Planetary Change*, **60**(3-4): 443–456. doi:[10.1016/j.gloplacha.2007.05.003](https://doi.org/10.1016/j.gloplacha.2007.05.003).
- Zimov, S. A., Y. Voropaev, I. Semiletov, S. Davidov, S. Prosiannikov, F. Chapin, M. Chapin, S. Trumbore and S. Tyler, 1997: North Siberian lakes: A methane source fueled by Pleistocene carbon. *Science*, **277**(5327): 800–802.
- Zimov, S. A., S. P. Davydov, G. M. Zimova, A. I. Davydova, E. A. G. Schuur, K. Dutta and F. S. I. Chapin, 2006: Permafrost carbon: Stock and decomposability of a globally significant carbon pool. *Geophysical Research Letters*, **33**(20): L20502. doi:[10.1029/2006GL027484](https://doi.org/10.1029/2006GL027484).

APPENDIX A: Downscaling Scheme

We employ the following scheme to expand the latitudinal zonal (mean) field of IGSM state or flux variables across the longitude (Schlosser *et al.*, 2012).

$$V_{x,y}^{IGSM} = \left(C_{x,y} + \frac{dC_{x,y}}{dT_{Global}} \Delta T_{Global} \right) \cdot V_y^{IGSM}, \quad C_{x,y}^{Obs/AR4} = \frac{V_{x,y}^{Obs/AR4}}{V_y^{Obs/AR4}} \quad (1)$$

where $V_{x,y}^{IGSM}$ and $V_{x,y}^{Obs/AR4}$ are transformed IGSM and any desired data set (observations or IPCC AR4 archive) at the longitudinal point (x) and given latitude (y), respectively; $C_{x,y}$ is the transformation coefficient for any reference or climatological time period under contemporary conditions, which basically reflects the relative value of any given variable at a longitudinal point in relation to its zonal mean; V_y^{IGSM} and $V_y^{Obs/AR4}$ are specific latitudinal zonal field of IGSM and any desired data set, respectively; derivative of the transformation coefficient $\frac{dC_{x,y}}{dT_{Global}}$ is the rate of transformation coefficient change with any human-forced global temperature change. It is calculated based on the difference in 10-year climatology of $C_{x,y}$ between the doubling of CO₂ in the IPCC SRES simulations at a transient rate of 1% per year (equivalent to 70 years) and the end of the 20th century in the transient CO₂ increase simulations (2xCO₂), then normalized by the global temperature difference of the same time period. ΔT_{Global} is the change in global temperature relative to the reference or climatological period. We examine the use of various SRES emissions scenarios (A2, A1B, B1) to calculate $\frac{dC_{x,y}}{dT_{Global}}$ and found a high degree of spatial consistency across these scenarios for all the seasons with their cross spatial-correlation coefficients mostly larger than 0.8 (Schlosser *et al.*, 2012). In this study we employ $\frac{dC_{x,y}}{dT_{Global}}$ calculated from climate simulations forced by the SRES A2 (17 climate models) emission scenario. The scheme is applied only to the precipitation, temperature, and radiation (longwave and shortwave) with other variables (surface pressure, specific humidity, and wind) simply taking the IGSM zonal mean across each longitudinal point along the latitude.

The transformation coefficients ($C_{x,y}$) at contemporary conditions are derived from multiple state-of-the-art observational datasets, including 31-year (1979-2009) climatology of the monthly GPCP v2.1 data set at 2.5° for precipitation (Huffman *et al.*, 2009), 27-year (1979-2005) climatology of the gridded land-only Climatic Research Unit (CRU) Time Series (TS) 3.0 at 0.5° for surface air temperature (Mitchell and Jones, 2005). Three other data sets are utilized to derive the shortwave and longwave radiation, including a 53-year (1948-2000) NCEP/NCAR corrected by CRU (NCC) forcing data set (Ngo-Duc *et al.*, 2005), a 57-year (1948-2004) forcing data set (Qian *et al.*, 2006), and the Global Offline Land-surface Dataset (GOLD) version 2 data set (Betts *et al.*, 2006). We compare the $C_{x,y}$ of the radiation calculated from the 22-year (1979-2000) climatology of all three forcing data sets and find small differences over most of areas. Therefore, the averaged values of $C_{x,y}$ are used in this study. Besides the derivative of the transformation coefficient determined by the 17 climate models from IPCC SRES A2 archive, we also examine the use of constant $C_{x,y}$ under contemporary conditions throughout the 21st century.

APPENDIX B: Temperature Dependence of Methane Ebullition Flux

The temperature dependency of methane ebullition flux is approximated by the empirical Q_{10} function as follows:

$$F = F_0 \cdot Q_{10}^{(T-T_0)/10} \quad (2)$$

The above relationship is applied for the yedoma and non-yedoma lakes, respectively. F is future methane ebullition flux in $\text{g CH}_4\text{m}^{-2}\text{yr}^{-1}$, F_0 is the methane ebullition flux in $\text{g CH}_4\text{m}^{-2}\text{yr}^{-1}$ under contemporary condition, which is based on > 16,000 measurements conducted at multiple sites in Alaska and Siberia (Walter *et al.*, 2006; Walter Anthony *et al.*, 2012). The averaged F_0 for non-yedoma lakes is $5.9 \text{ g CH}_4\text{m}^{-2}\text{yr}^{-1}$. For yedoma lakes, flux number ($139 \text{ g CH}_4\text{m}^{-2}\text{yr}^{-1}$) at the thermokarst fringe of yedoma lakes (i.e. ebullition survey areas running perpendicular ~ 50 m from a thermokarst shore towards the lake center) is used, which represents ebullition from yedoma land areas that will become yedoma lakes in the future. Q_{10} takes the value of 3.0. Since CLM does not simulate the lake dynamics, we use the soil temperature at around 2m depth (layer 9) instead. Layered soil temperatures are obtained from the off-line CLM simulations driven by the downscaled IGSM forcings. T_0 takes 2003-2009 climatology of 2-meter soil temperature under the IGSM forcing with median TCR and median emission parameters (MTCR run). T is the soil temperature of the same depth under various climate projections. The temperature is averaged for multiple grids corresponding to the multiple field locations of Alaska and Siberia. The resulting methane ebullition fluxes for yedoma and non-yedoma lakes will change annually from 2010 throughout the 21st century.

APPENDIX C: IGSM Estimated Human Global CH₄ Emissions

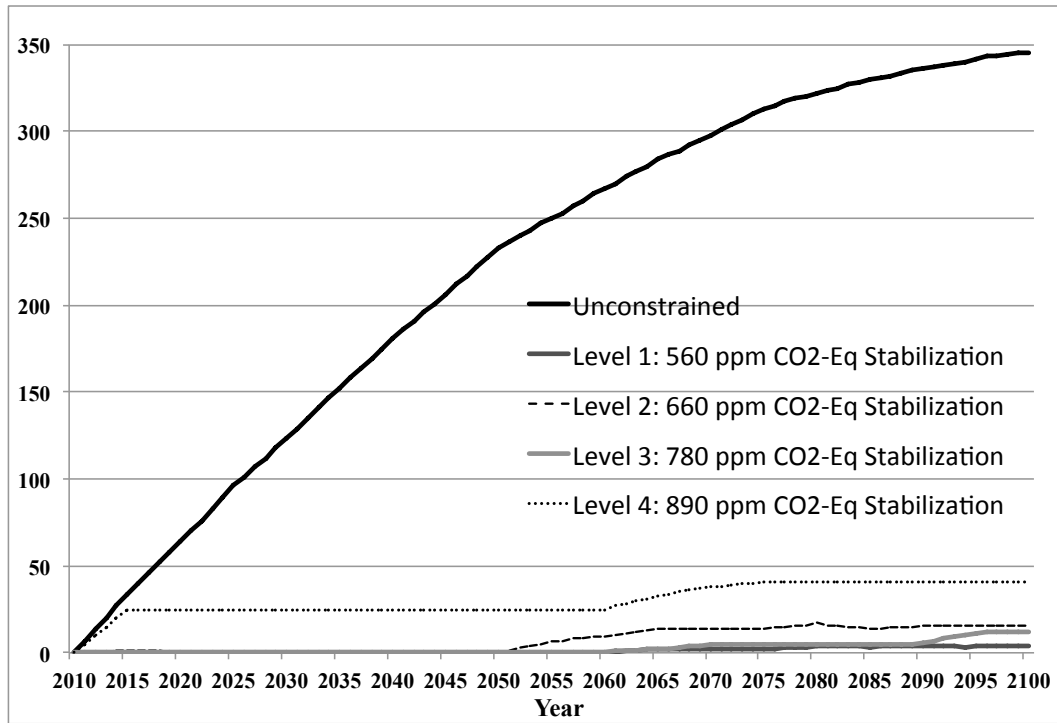


Figure C1. Changes in the IGSM estimated human global CH₄ emissions (Tg-CH₄yr⁻¹) under various climate policy scenarios. Global emissions are 345 Tg-CH₄yr⁻¹ at 2010 and increases by 349 and 4 Tg-CH₄yr⁻¹ under the UCE and GST scenarios, respectively.

APPENDIX D

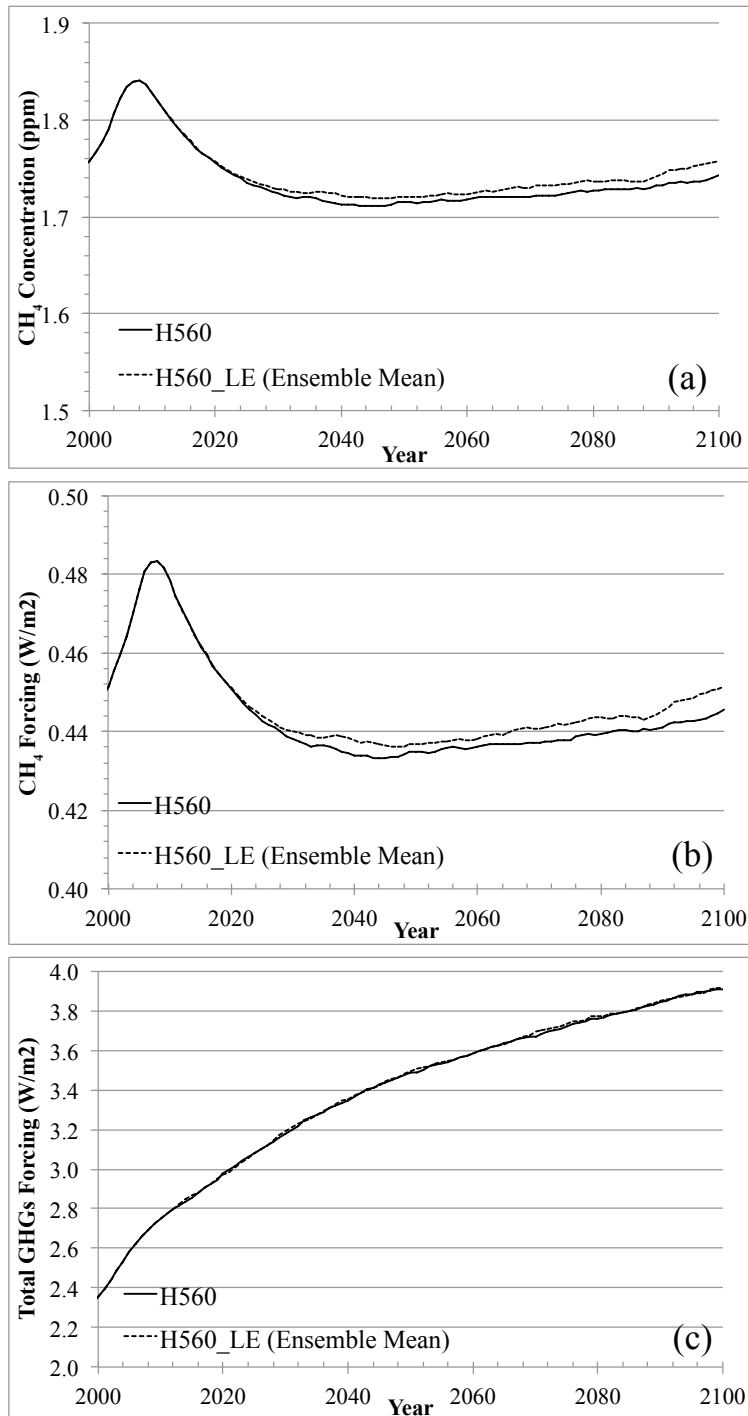


Figure D1. The IGSM-estimated a) CH₄ concentration (ppm), b) CH₄ forcing (W/m²), and c) Total greenhouse gas (GHGs) forcing (W/m²) without and with the increased lake CH₄ emissions for the HTCR case under the GST scenario. As can be seen, a 1% increase of CH₄ concentration has a very minor effect on radiative forcing.

REPORT SERIES of the MIT Joint Program on the Science and Policy of Global Change

FOR THE COMPLETE LIST OF JOINT PROGRAM REPORTS:
<http://globalchange.mit.edu/pubs/all-reports.php>

174. **A Semi-Empirical Representation of the Temporal Variation of Total Greenhouse Gas Levels Expressed as Equivalent Levels of Carbon Dioxide** *Huang et al.* June 2009
175. **Potential Climatic Impacts and Reliability of Very Large Scale Wind Farms** *Wang & Prinn* June 2009
176. **Biofuels, Climate Policy and the European Vehicle Fleet** *Gitiaux et al.* August 2009
177. **Global Health and Economic Impacts of Future Ozone Pollution** *Selin et al.* August 2009
178. **Measuring Welfare Loss Caused by Air Pollution in Europe: A CGE Analysis** *Nam et al.* August 2009
179. **Assessing Evapotranspiration Estimates from the Global Soil Wetness Project Phase 2 (GSWP-2) Simulations** *Schlosser and Gao* September 2009
180. **Analysis of Climate Policy Targets under Uncertainty** *Webster et al.* September 2009
181. **Development of a Fast and Detailed Model of Urban-Scale Chemical and Physical Processing** *Cohen & Prinn* October 2009
182. **Distributional Impacts of a U.S. Greenhouse Gas Policy: A General Equilibrium Analysis of Carbon Pricing** *Rausch et al.* November 2009
183. **Canada's Bitumen Industry Under CO₂ Constraints** *Chan et al.* January 2010
184. **Will Border Carbon Adjustments Work?** *Winchester et al.* February 2010
185. **Distributional Implications of Alternative U.S. Greenhouse Gas Control Measures** *Rausch et al.* June 2010
186. **The Future of U.S. Natural Gas Production, Use, and Trade** *Paltsev et al.* June 2010
187. **Combining a Renewable Portfolio Standard with a Cap-and-Trade Policy: A General Equilibrium Analysis** *Morris et al.* July 2010
188. **On the Correlation between Forcing and Climate Sensitivity** *Sokolov* August 2010
189. **Modeling the Global Water Resource System in an Integrated Assessment Modeling Framework: IGSM-WRS** *Strzepek et al.* September 2010
190. **Climatology and Trends in the Forcing of the Stratospheric Zonal-Mean Flow** *Monier and Weare* January 2011
191. **Climatology and Trends in the Forcing of the Stratospheric Ozone Transport** *Monier and Weare* January 2011
192. **The Impact of Border Carbon Adjustments under Alternative Producer Responses** *Winchester* February 2011
193. **What to Expect from Sectoral Trading: A U.S.-China Example** *Gavard et al.* February 2011
194. **General Equilibrium, Electricity Generation Technologies and the Cost of Carbon** *Abatement Lanz and Rausch* February 2011
195. **A Method for Calculating Reference Evapotranspiration on Daily Time Scales** *Farmer et al.* February 2011
196. **Health Damages from Air Pollution in China** *Matus et al.* March 2011
197. **The Prospects for Coal-to-Liquid Conversion: A General Equilibrium Analysis** *Chen et al.* May 2011
198. **The Impact of Climate Policy on U.S. Aviation** *Winchester et al.* May 2011
199. **Future Yield Growth: What Evidence from Historical Data** *Gitiaux et al.* May 2011
200. **A Strategy for a Global Observing System for Verification of National Greenhouse Gas Emissions** *Prinn et al.* June 2011
201. **Russia's Natural Gas Export Potential up to 2050** *Paltsev* July 2011
202. **Distributional Impacts of Carbon Pricing: A General Equilibrium Approach with Micro-Data for Households** *Rausch et al.* July 2011
203. **Global Aerosol Health Impacts: Quantifying Uncertainties** *Selin et al.* August 2011
204. **Implementation of a Cloud Radiative Adjustment Method to Change the Climate Sensitivity of CAM3** *Sokolov and Monier* September 2011
205. **Quantifying the Likelihood of Regional Climate Change: A Hybridized Approach** *Schlosser et al.* October 2011
206. **Process Modeling of Global Soil Nitrous Oxide Emissions** *Saikawa et al.* October 2011
207. **The Influence of Shale Gas on U.S. Energy and Environmental Policy** *Jacoby et al.* November 2011
208. **Influence of Air Quality Model Resolution on Uncertainty Associated with Health Impacts** *Thompson and Selin* December 2011
209. **Characterization of Wind Power Resource in the United States and its Intermittency** *Gunturu and Schlosser* December 2011
210. **Potential Direct and Indirect Effects of Global Cellulosic Biofuel Production on Greenhouse Gas Fluxes from Future Land-use Change** *Kicklighter et al.* March 2012
211. **Emissions Pricing to Stabilize Global Climate** *Bosetti et al.* March 2012
212. **Effects of Nitrogen Limitation on Hydrological Processes in CLM4-CN** *Lee & Felzer* March 2012
213. **City-Size Distribution as a Function of Socio-economic Conditions: An Eclectic Approach to Down-scaling Global Population** *Nam & Reilly* March 2012
214. **CliCrop: a Crop Water-Stress and Irrigation Demand Model for an Integrated Global Assessment Modeling Approach** *Fant et al.* April 2012
215. **The Role of China in Mitigating Climate Change** *Paltsev et al.* April 2012
216. **Applying Engineering and Fleet Detail to Represent Passenger Vehicle Transport in a Computable General Equilibrium Model** *Karplus et al.* April 2012
217. **Combining a New Vehicle Fuel Economy Standard with a Cap-and-Trade Policy: Energy and Economic Impact in the United States** *Karplus et al.* April 2012
218. **Permafrost, Lakes, and Climate-Warming Methane Feedback: What is the Worst We Can Expect?** *Gao et al.* May 2012